

Sediment Extraction and Flow Structure of Vortex Settling Basin

Jafar Chapokpour and Javad Farhoudi

Department of Irrigation and Reclamation Eng.,
College of Agricultural Eng. and Technology, University of Tehran, Karaj, Iran

Abstract: The paper presents the results of an investigation conducted in a vortex chamber to observe flow structure as well as extraction efficiency. During the experiments, various flow discharges were employed with high flow entrance velocities. Three sizes of sediment were fed at three different rates. It was observed that the increase in the flow and sediment feeding rates result in the increase of sediment extraction efficiency of the settling basin. A Son Tek 50Hz ADV velocity measuring equipment was utilized to determine flow structure inside the basin under clear water condition. It was also found that various types of flow patterns were developed in radial sections which may play a positive or negative role in sediment trapping process. The tangential and radial velocities were analyzed in various horizontal sections and it was observed that generally the helical motion path length of sediment particles towards the central flushing orifice in lower sections is longer than upper sections.

Key words: Sediment extraction • Vortex chamber • Extraction efficiency • Flow structure

INTRODUCTION

Sediment deposition in diversion canals is one of the most severe problems which the designers and operators are often faced with. Sediment laden flows are capable to transport and deposit a considerable rate of sediment load in the conveyance channels which results in reduction of conveyance capacity of the system. Therefore, measures are to be taken to exclude the sediment particles from the diverted flow into the irrigation canals. Different types of sediment extractors/excluders, such as tunnel type, vortex tubes, rectangular settling basins and vortex type settling basins are often employed for this purpose. In recent years the vortex settling basin (VSB) has attracted a considerable interest among the water engineers. The vortex settling basin (VSB), is a continuous device which applies a certain fraction of flow for flushing the sediment particles out of the diverted stream [1]. Classical settling basins generally suffer from two main disadvantages: (i) requirement of large dimensions of basin compared with other types and (ii) longer settling time for sediment particles. Sediment extractors of vortex type would overcome the mentioned disadvantages [2]. VSB utilizes centrifugal forces to generate a vortex motion around its central axis to remove sediment particles from the incoming flow by means of secondary currents in the chamber through the central flushing orifice [3]. In this

device the high velocity flow is introduced tangentially into cylindrical basin having an orifice at the center of its bottom. This gives rise to the combined vortex conditions (Rankine type) having a forced vortex near the orifice and a free vortex at the outer region towards the periphery of the basin. As a result, sediment concentration gradient builds up across the vortex and a diffusive flux, proportional but opposite to the centrifugal flux, is induced [4]. Resulting secondary flow causes the flow layers adjacent to the floor of the basin moving towards the central outlet orifice. Therefore, the sediment particles reaching the center of the chamber could be flushed out continuously through the orifice and a relatively sediment free water would leave the basin through its overflow weir crest [5]. The vortex settling basins have been investigated principally by Vokes and Jenkines (1943), Velioglu (1972), Salakhov (1975), Cecen and Bayazit (1975), Sullivan *et al.*, (1978), Curi *et al.*, (1979), Mashuri (1981,1986), Svarovski (1981), Ogihara and Sakagouchi (1984), Sanmogatant (1985), Zhou *et al.*, (1989, 1997), Paul *et al.*, (1991), Ziaei (2000, 2001), Athar *et al.*, (2002, 2003), Keshavarzi and Gheisi (2006) [2].

The summary of these investigations is given in Tables 1 and 2. In their experimental studies the investigators tried to focus on the trap efficiency of the vortex settling basin and express an appropriate relationship for its estimation.

Table 1: Range of sediment size used in previous studies [2]

Authors	Range of sediment size (mm)
Curi <i>et al.</i> , (1977)	2.12
Mashauri M-1 (1986)	0.375-1.80
Mashauri M-2 (1986)	0.18-0.75
Mashauri M-3 (1986)	0.063-0.25
IPRI (1989)	0.09-0.30
Paul <i>et al.</i> , M-1 (1991)	0.175
Paul <i>et al.</i> , M-2 (1991)	0.05-1.00
Paul <i>et al.</i> , M-3 (1991)	7.64
Ziaei (2000)	0.07-0.9
Athar <i>et al.</i> , (2002)	0.055-0.931
Keshavarzi and Gheisi (2006)	0.075-0.3

Table 2: Previously published main relationships [2]

Investigator	Relationships
(1) Curi <i>et al.</i> , (1977)	$\eta_o = 1.74 + \ln \left[\frac{d_o^{0.11} \times (\gamma_s / \gamma_f)^{0.88}}{Q_i^{0.58}} \right]$
(2) Mashuri (1986)	$\eta_o = 0.835 - \frac{0.0292}{k_1} + 1.71 \times 10^{-2} \times \frac{d}{d_o} - 5.93 \times 10^{-4} \times \frac{d}{d_o \times k_1}$
(3) Paul <i>et al.</i> , (1991)	$a) \eta_o = 73.4 + 8 \times \log \left(\frac{\omega}{W} \right) \quad b) \eta_o = 2.16 \times \left(\frac{\omega}{V_{to}} \right)^{0.04} \times \left(\frac{Q_o}{Q_i} \right)^{1.27}$ $c) \eta_o = 98 + 0.92 \times \log \left(\frac{\omega}{W} \right) \quad d) \eta_o = 97.8 \times \left(\frac{\omega}{V_{to}} \right)^{0.0045} \times \left(\frac{Q_o}{Q_i} \right)^{0.01}$
(4) Athar <i>et al.</i> , (2002)	$\eta_o = k_o \times \left(\frac{Q_o}{Q_i} \right)^{0.25} \times \left(\frac{Z_h}{h_p} \right)^{0.35} \times \left(\frac{\omega \times d_{50}}{v} \right)^{0.15} \times \left(\frac{Q_w^2}{g \times R^3 \times h_p^2} \right)^{0.11}$

Where: B = width of the inlet canal (m), d = diameter of the basin (m), d_o = diameter of central orifice (m),

h_p = depth of flow at the periphery of vortex basin (m), k_1 = mobility factor, k_o = coefficient related to the configuration of vortex settling basin, L_f = length of overflow weir (m), Q_i = entrance flow discharge (m³/s),

Q_o = flushing discharge (m³/s), $Q_w = Q_o + K \cdot Q_s$ = weighted discharge (m³/s), Q_s = overflow discharge (m³/s),

R = radius of basin (m), V_{to} = tangential velocity at $r = r_o$ (m/s), $W = 4Q_s/\pi d^2$ = vertically upward velocity at center of basin (m/s), Z_h = difference between bed levels of overflow weir and vortex basin (m), γ_f = specific weight of fluid (N/m³), γ_s = specific weight of sediment particles (N/m³), η_o = removal efficiency of vortex settling basin (%), v = kinematics viscosity of fluid (m²/s), ω = fall velocity of sediment particles in quiescent water (m/s)

In general, the previous studies faced with some constraints such as steady state rate of sediment feeding into flow reach, sediment collection from the central orifice, sediment deposition on the deflector and entrance diaphragm. The lack of knowledge about the mechanism, structure and state of generated secondary currents in the basin was also one of the problems that the previous works were faced with. Keshavarzi and Gheisi [2], designed a point feeder type of sediment and a device for its collection from the flushing orifice. The device may be subjected to some disadvantages because of its point feeding type.

The sediment feeder that was used by Ziaei [3], consists of a funnel wise hopper for sediment storage, a

movable forked plate installed beneath the slot of the hopper and a guide plate with adjustable slope. The sediment particles were released from the hopper through the slot onto the guide plate which was shacked by an electro-motor. The sediment rate was controlled by variation of the speed of electro-motor, slope of the moveable plate and its distance from the slot of the hopper. It is noteworthy to mention that the sediment rate was highly unsteady in this device.

Athar *et al.* [4] used a cylindrical sediment feeding device which maintained the sediment in the basin as bed load. The recommended device was subjected to unsteady feeding rate where a great amount of sediment was carried adjacent to the bed level.

Table 3: Characteristics of settling basin

Height of chamber $H(m)$	Diameter of central orifice $d_o(m)$	Type of overflow weir	Length of overflow weir $L_1 (m)$	Diameter of chamber $d (m)$	Basin depth at periphery $h_2 (m)$	Width of inlet channel $B(m)$	Length of inlet channel (m)	Slope of inlet channel $S\%$
0.7	0.075	circular overflow weir	0.8	1.5	0.06	0.3	6	0.045

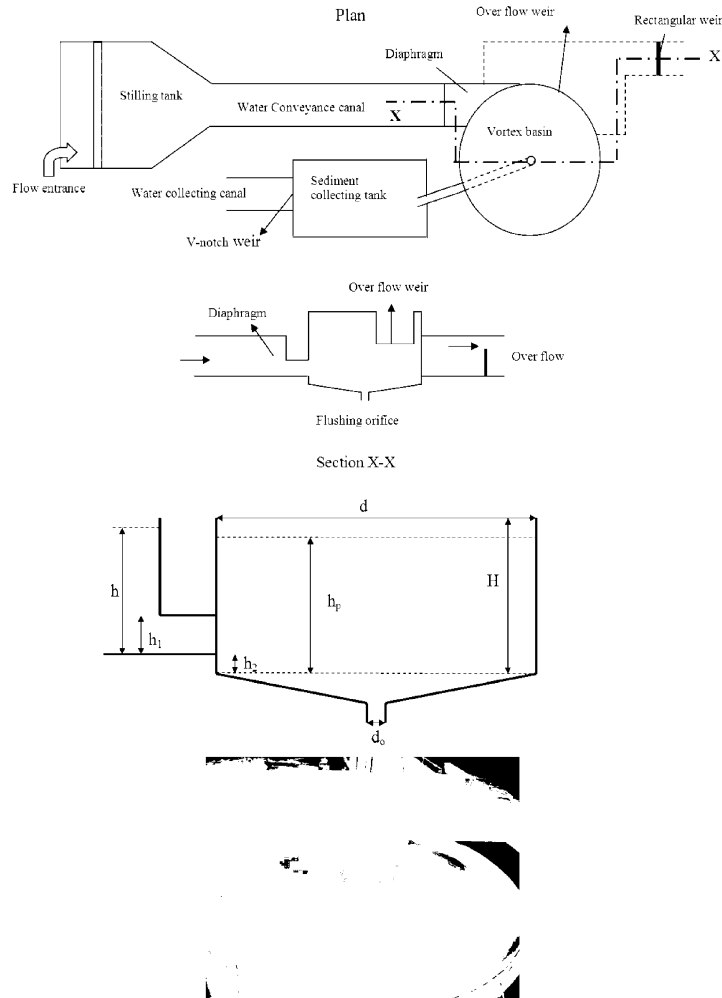


Fig. 1: Schematic layout and parameters of vortex settling basin

Keshavarzi and Gheisi [2] designed a new equipment based on the sand clock to provide a steady rate of sediment feeding into the inlet flow. The device was a point feeder type in which the sediment particles would be distributed non-uniformly across the channel reach.

In the present study, the diaphragm and the deflector were eliminated to solve the problem of sediment deposition on their top surfaces. Despite the other investigators, the height of the entrance orifice was decreased by 30% which resulted in a high velocity of entrance flow jet.

A strip type sediment feeder was employed throughout the experiments to overcome the disadvantages of unsteady feeding and point feeding of sediments recommended by the previous researches.

To understand the flow structure, in horizontal and radial sections of the basin, series of flow measurement readings were recorded.

Experimental Layout and Methodology: The experiments were carried out in a physical model of the vortex settling basin with the characteristics shown in Table 3 and schematically depicted in Fig. 1.

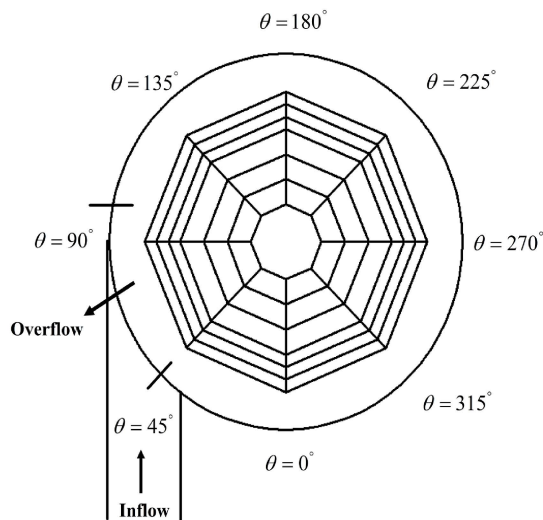


Fig. 2: Radial sections for velocity measurement with location of entrance and overflow weir

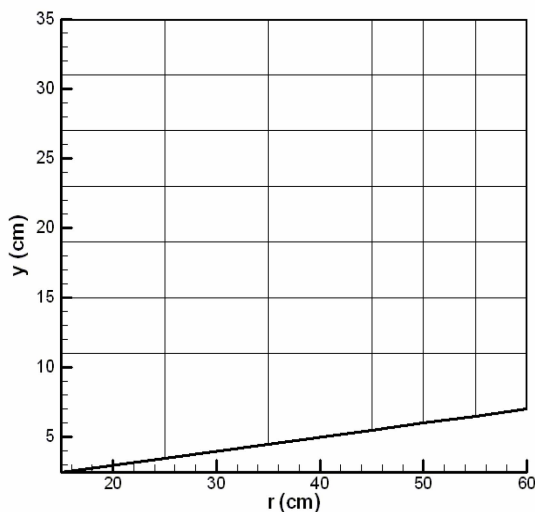


Fig. 3: Grid of data collection in each radial section

The tests were performed in a configuration in which the angular distance of inlet and overflow outlet was 0 degree as recommended by Paul *et al.* [6]. To maintain a tangential inlet flow jet in the vortex basin, a diaphragm was installed across the entrance channel at a level of 0.12m from the canal bed. Water was then supplied from a constant head tank connected through upstream stilling tank to the circulating water supply system of the laboratory where the incoming flow was regulated by means of a turning valve. Precautions were made to avoid large eddies and disturbances at the free surface of water in the upstream stilling tank. Also some fiber bags were used for collection of the sediment particles as proposed by Keshavarzi and Gheisi [2].

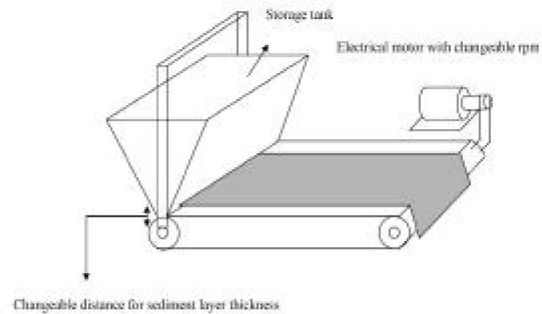


Fig. 4: Schematic diagram of sediment feeder used in this research

The discharge from overflow weir and flushing orifice were measured by means of a pre-calibrated sharp crested rectangular weir and a V-notch respectively.

An Acoustic Doppler Velocity meter (ADV) was used to measure the flow velocities in three dimensions to determine the dominant secondary currents inside of the vortex basin.

The velocities were measured in eight radial sections at intervals of 45° from the origin, as shown in Fig. 2.

At each radial section, 56 points were selected in a grid of velocity measurement, as demonstrated in Fig. 3, resulting in a total of 448 measuring points inside the chamber.

Design of New Sediment Feeder: A sediment feeder was designed and used to overcome the disadvantages focused on the previous devices. It consists of a sediment storage tank with a cross slot at its bottom riding on a conveyer belt which was operated by an electro-motor with adjustable rpm. The sediment feeding rate was regulated by changing the distance between the slot and conveyer belt along with the adjustment of electro motor's rpm. The feeder then was installed on the top of the inlet canal to distribute a uniform rate of sediment particles across the entrance canal. The schematic diagram of sediment feeder is shown in Fig. 4.

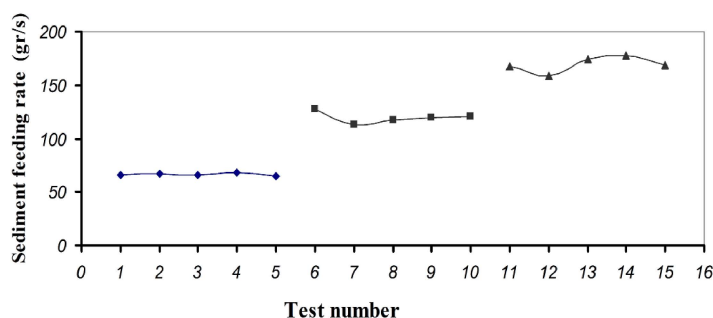


Fig. 5: Typical feeder calibration curve with different durations for $d_{50}=0.55$ mm

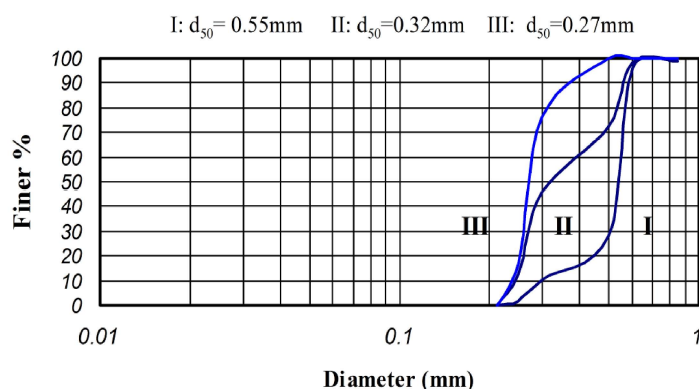


Fig. 6: The size distribution of sediments

The calibration of sediment feeder was achieved by conducting 45 experiments with three speeds of electro motor, five time lengths and three sediment sizes. The angular velocities of 20, 40 and 60 rpm were selected to maintain three sediment feeding rates of 67 (gr/s), 120 (gr/s) and 170 (gr/s). The typical calibration curve for each sediment size is illustrated in Fig. 5.

Experimental Program: Sediment removal efficiency of vortex sediment extractor was measured under three entrance discharges of 20.97(l/s), 30.97(l/s) and 34.38(l/s). Three non cohesive sediments having uniform sediment sizes of $d_{50}=0.55$ mm, $d_{50}=0.27$ mm and a non uniform size of $d_{50}=0.32$ mm with relative density of 2.65 were used. The size distribution of used sediments is illustrated in Fig. 6. At the beginning of each experiment the flow was admitted into the chamber for 10 minutes to maintain an equilibrium flow state all over the system. The sediment was then fed into the chamber until reaching equilibrium inside the chamber. The fiber bag was installed under the central orifice outlet to collect the extracted sediment particles in the chamber in duration of 15 minutes and the collected sediments were then dried and weighted.

The removal efficiency and hydraulic efficiency throughout the experiments were defined and calculated respectively as:

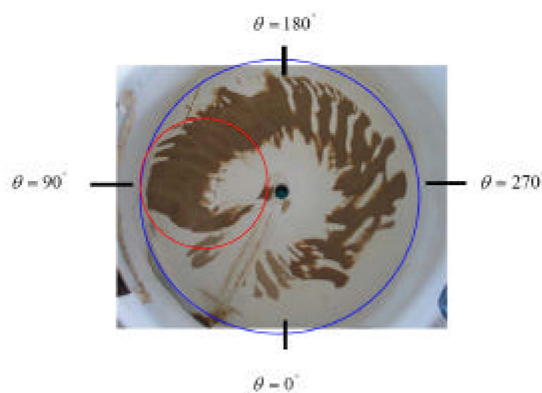


Fig. 7: The configuration of sediment deposition thickness on the basin bed

$$\eta_o = \frac{\omega_o}{\omega_i} \times 100$$

$$\eta_h = \left(1 - \frac{Q_o}{Q_i}\right) \times 100 \quad (1)$$

Where:

- η_o = Removal efficiency of the basin
- ω_o = Dry weight of the sediment, flushed out through the bottom orifice
- ω_i = Weight of sediment fed into the basin
- η_h = Hydraulic efficiency of the basin
- Q_o = Discharge from bottom orifice and
- Q_i = Inlet discharge to the basin

Table 4: Experimental conditions and results of tests

Test number	Inlet discharge (l/s)	Overflow discharge (l/s)	Bottom orifice discharge (l/s)	Sediment median size d_{50} (mm)	Sediment feeding rate (g/s)	Hydraulic efficiency %	Trap efficiency %
1	20.97	17.99	2.98	0.55	67	85.8	45
2	20.97	17.99	2.98	0.55	120	85.8	48
3	20.97	17.99	2.98	0.55	170	85.8	50
4	30.97	28.49	2.48	0.55	67	92.0	94
5	30.97	28.49	2.48	0.55	120	92.0	92
6	30.97	28.49	2.48	0.55	170	92.0	92
7	34.38	32.06	2.32	0.55	67	93.2	88
8	34.38	32.06	2.32	0.55	120	93.2	90
9	34.38	32.06	2.32	0.55	170	93.2	90
10	20.97	17.99	2.98	0.32	67	85.8	63
11	20.97	17.99	2.98	0.32	120	85.8	53
12	20.97	17.99	2.98	0.32	170	85.8	43
13	30.97	28.49	2.48	0.32	67	92.0	85
14	30.97	28.49	2.48	0.32	120	92.0	88
15	30.97	28.49	2.48	0.32	170	92.0	88
16	34.38	32.06	2.32	0.32	67	93.2	80
17	34.38	32.06	2.32	0.32	120	93.2	83
18	34.38	32.06	2.32	0.32	170	93.2	84
19	20.97	17.99	2.98	0.27	67	85.8	55
20	20.97	17.99	2.98	0.27	120	85.8	58
21	20.97	17.99	2.98	0.27	170	85.8	64
22	30.97	28.49	2.48	0.27	67	92.0	78
23	30.97	28.49	2.48	0.27	120	92.0	81
24	30.97	28.49	2.48	0.27	170	92.0	82
25	34.38	32.06	2.32	0.27	67	93.2	70
26	34.38	32.06	2.32	0.27	120	93.2	77
27	34.38	32.06	2.32	0.27	170	93.2	78

RESULTS AND DISCUSSIONS

Removal Efficiency of the Basin: Referring to the flow conditions shown in Table. 4 and Fig. 8, it was observed that the removal efficiency of vortex settling basin with $d_{50}=0.55$ mm is higher than two other sediment sizes, having the biggest magnitude of 94 percent because of high fall velocity rather than two others and acting as bed load inside the chamber. Also with finer sediment sizes of $d_{50}=0.32$ and $d_{50}=0.27$ mm, the best removal efficiency was 88% and 82% respectively. It is noted that, under $Q_i=20.97$ (l/s) and entrance velocity=0.6 m/s, the thickness of deposited sediment layer on the basin floor follows a spatial pattern which pertain a thick deposited layer in the angular distance between 90° and 135° and a thinner thickness between 225° and 315° as is shown in Fig. 7.

Generally the removal efficiency of the basin was increased in accordance with the rate of entrance discharge so that when the flow rate was adjusted to $Q_i=30.97$ (l/s) with entrance velocity= 0.86 (m/s), the best

removal efficiency equal to 94 percent was obtained. However, it was observed that when the entrance discharge increased to 34.38 (l/s), the removal efficiency of the chamber was slightly decreased unlike the foregoing conclusions which could be attributed to the presence of turbulence in the chamber disturbing the free water surface and leading sediment particles towards the overflow current.

It would be concluded that the higher entrance velocities enforce the particles to circulate inside the basin and decreases the influence of overflow weir jet to transport the sediment load by weir flow. Because of helical motion existence, it was observed that the trapping opportunity during the second circulation, around the basin centre, is more than the first circulation. This is due to the longer distance between sediment particle and overflow jet in the second circulation (Fig. 12).

It was also observed that, the removal efficiency of the basin was increased as the sediment feeding rates increased from 67 to 170 (gr/s).

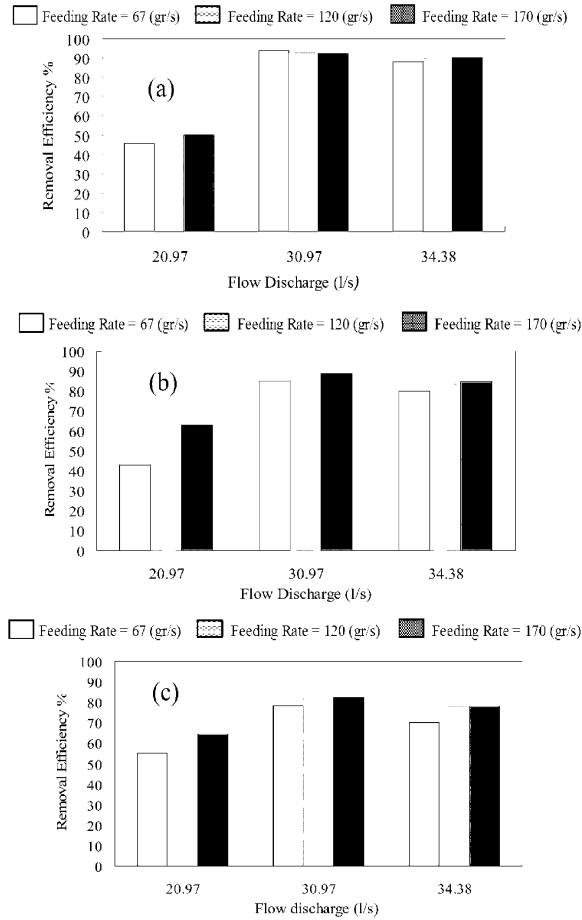


Fig. 8: Removal efficiency of vortex settling basin under three sediment feeding rates and three flow discharges. (a) uniform grain size with $d_{50} = 0.55$ mm. (b) non uniform grain size with $d_{50} = 0.32$ mm. (c) uniform grain size with $d_{50} = 0.27$ mm

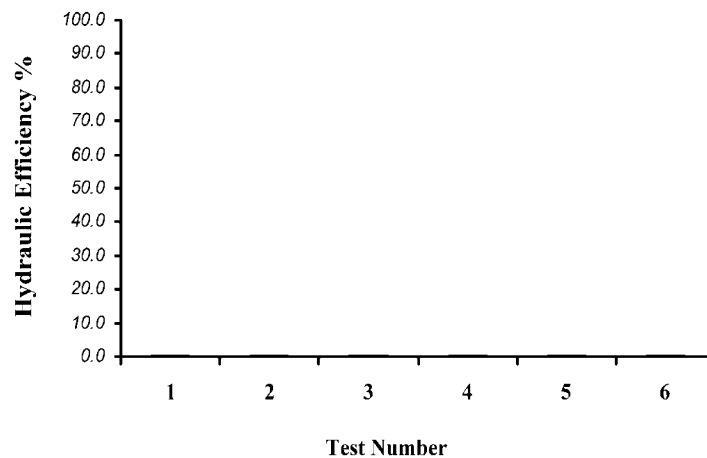


Fig. 9: Observed hydraulic efficiency of vortex basin

As is illustrated in Table 4, hydraulic efficiency of basin (η_h) is enhanced by increasing of entrance flow. For more exhibitions, Another Six experiments under increasing entrance discharge condition from 13.6(l/s) to 41(l/s) were accomplished (Fig. 9). It was observed that as the incoming discharge increased the central air core expanded (Fig. 10), decreasing flushing discharge, resulting lower flushing discharge and higher hydraulic efficiency.

During the whole experiments it was noted that, the central air core was formed completely from water surface towards central flushing orifice having a ring shaped outlet flow from bottom orifice which becomes smaller, in ring diameter, as the discharge increases. It is noteworthy to mention that in higher discharges larger than 41(l/s), semi-helical displacement of air core was occurred around the central orifice disturbing the flow inside of basin.

Literature review showed that, several relationships were recommended by various investigators to estimate the removal efficiency of vortex settling basin (Table 2), which were widely studied by Athar *et al.* [4] who concluded a general relationship. His recommended expression could correlate the experimental records of removal efficiency in a vortex chamber and field observations within the range of $\pm 40\%$ errors.

The following relationships suggested by Paul *et al.* [6] and Athar *et al.* [4] respectively, (Table 2) were examined in this research and the results depicted in Fig. 11. The results show an acceptable agreement with there relationships at the above mentioned range of accuracy.



Fig. 10: Expansion and propagation of central air core

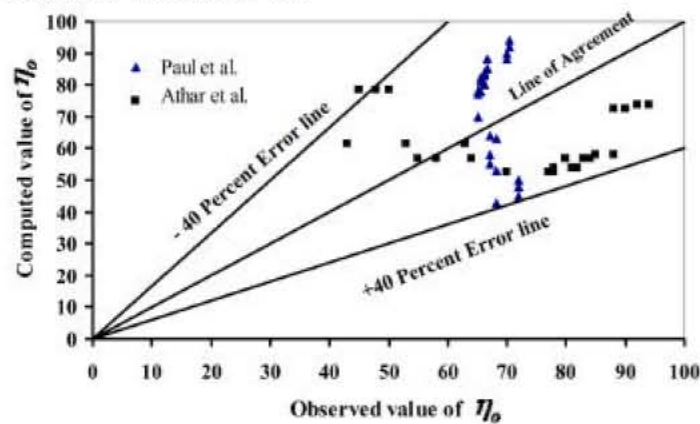


Fig. 11: Comparison between observed and computed values of removal efficiency

$$\eta_o = 73.4 + 8 \times \log \left(\frac{\omega}{W} \right) \quad (2)$$

$$\eta_o = k_o \times \left(\frac{Q_o}{Q_i} \right)^{0.25} \times \left(\frac{Z_h}{h_p} \right)^{0.35} \times \left(\frac{\omega \times d_{50}}{v} \right)^{0.15} \times \left(\frac{Q_w^2}{g \times R^3 \times h_p^2} \right)^{0.11} \quad (3)$$

Flow Characteristics: Secondary currents were generated in the vortex settling basin as a consequences of the effects raised from (i) entering water jet, (ii) over fall water jet from the curved weir crest and (iii) the bed slope of the basin towards the central orifice. To realize the characteristics of secondary currents in radial sections and its influences on removal efficiency, the velocity measurements in radial sections were analyzed and

streamlines depicted in Fig. 12 from which the followings outlines could be mentioned:

- At the radial section of 0° , the dominant vortex is in clockwise direction mood and located between radial distances of 0 to 50cm from the center of basin. This vortex, with a circulation tendency towards the central air core and flushing pipe, had a great influence on the sediment movement near the bed floor trapping nearly all sediment particles there. On the other hands, in the regions near to sidewall a weak tendency for anticlockwise (vortex) was observed.
- In the radial section of 45° , clockwise vortex was disappeared.

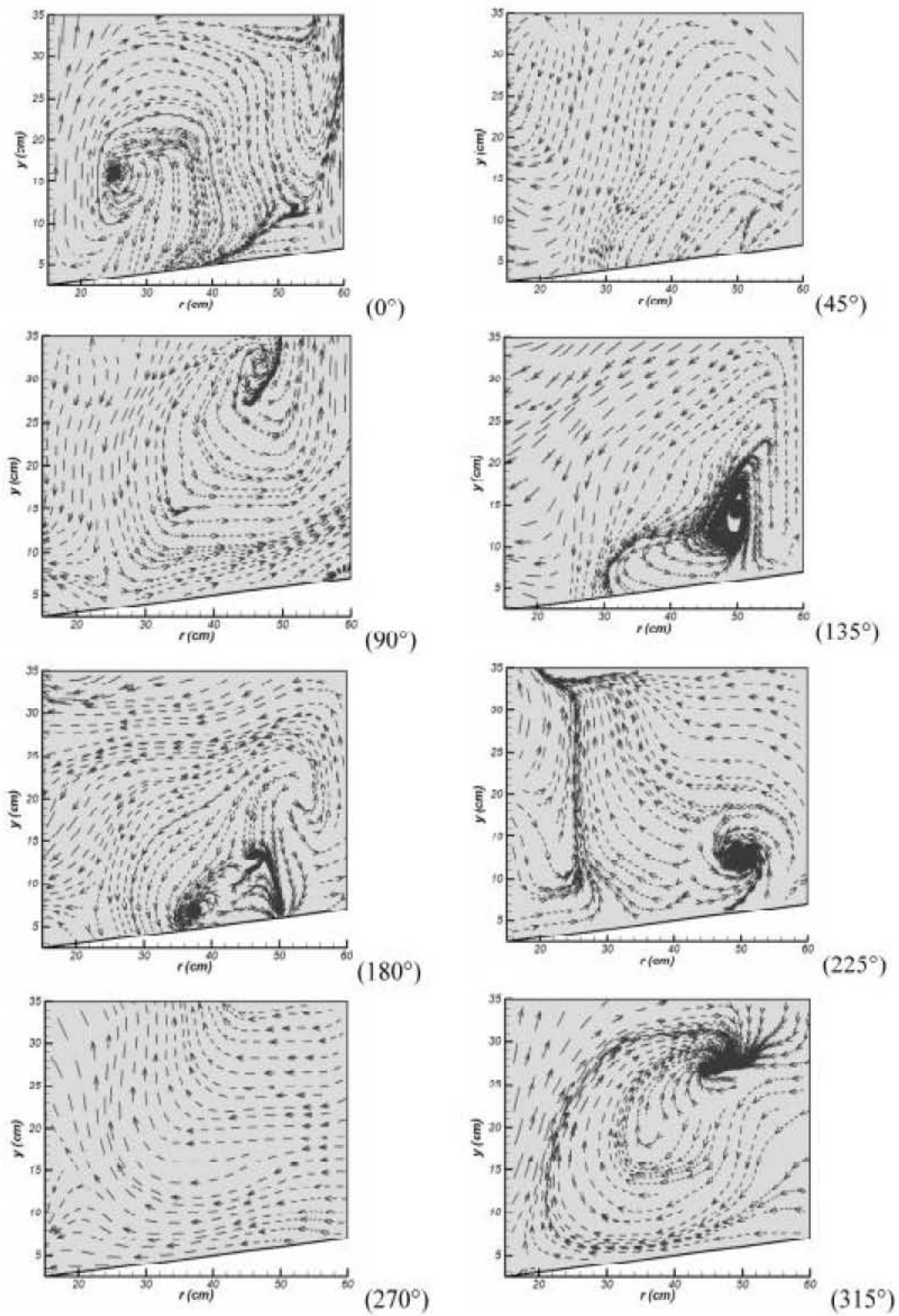


Fig. 12. Flow streamlines at different radial sections.

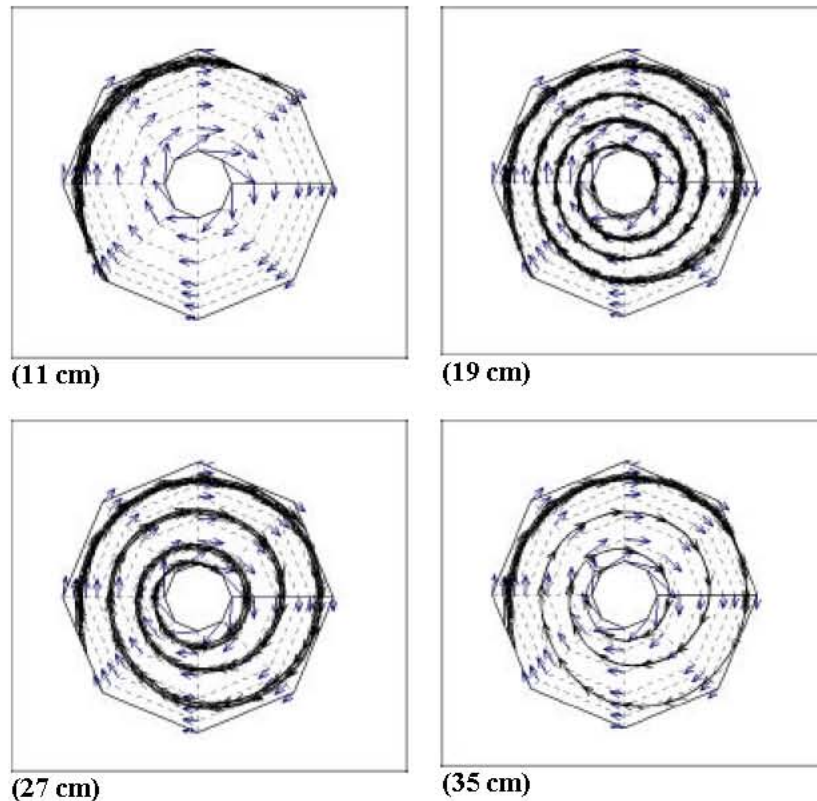


Fig. 13: Velocity vectors and flow streamlines at different

- In the radial section of 90° , anticlockwise vortex is generated. In this section the streamlines followed by the anticlockwise vortex with its direction from center to the sidewall. Consequently, the sediment particles were moved from the centre of basin towards the sidewall depositing denser sediment layer adjacent to the wall.
- In the radial section of 135° , the powerful center of anticlockwise vortex is located at the lower depths having a dominant propagation of currents towards the central air core.
- In the radial section of the 180° , the secondary currents generally were extended towards the central air core showing the circulation of weak anticlockwise vortex and a sink near the basin bed.
- At the radial section of 225° , propagation of currents in the direction of water surface was noted where a circulating anticlockwise vortex core existed between radial distance of 45 to 55 cm.
- At the radial section of 270° , it was found that the anticlockwise vortex diminished and currents were dominantly extended towards the central air core.
- At the radial section of 315° , the generation of a sink-vortex was observed, having clockwise

circulation absorbing most of the streamlines with a positive role in trapping of sediments particles.

Based on the above mentioned analyzes in considering the generation, extension, weakening and directions of flow patterns it was found that at the region of 225° to 315° , the highest trapping action was performed which falls in a good agreement with experimental observations for sediment deposition in the basin (Fig. 7).

The tangential and radial velocities were measured and analyzed from which the velocity vectors and flow streamlines were constructed at superimposed horizontal sections as is depicted in Fig. 13 (4 typical sections are showed), where the vertical distance between two consecutive sections was 4 cm. Generally it was found that the direction of streamlines are towards the side wall of basin in lower sections which tends the sediment particles travel a longer path towards the central orifice as bed load. Whereas, in the upper sections the sediment particles take a shorter paths towards the central air core as suspended load.

Two dimensional velocity vector analysis in the horizontal sections, showed that the velocity adjacent to

zones of central air core is higher than those on other zones maintaining a constant magnitude near the side walls of the chamber. Despite to this observation, at the radial line of 90° from origin and zones near the entrance flow jet, velocity vectors were influenced by entrance flow jet showing an increasing magnitude by nearing to the sidewall.

CONCLUSIONS

In general, by increasing the entering discharge and sediment feeding rate the removal efficiency of the basin becomes larger. Therefore, unlike classical settling basins the vortex settling basin needs for higher inlet velocity to maintain a higher efficiency.

Decreasing the level of entrance orifice by 30% from that of proposed by Paul *et al.* [6], increases the entrance velocity, without having a deflector, which would result in a solution for the problem of sediment deposition on the top surface of deflector.

An increase in the incoming velocity generates a powerful centrifugal forced vortex causing a better formation of central air core with smaller flushing ring diameter which results in higher hydraulic efficiencies of the basin.

Based on velocity analysis, it was noted that in the lower flow layers the sediment particles take a longer helical path towards flushing orifice with a higher concentration of sediment around flushing orifice, rather than upper flow layers.

The secondary currents in radial sections have various flow patterns in the basin which may impose either positive or negative role in sediment trapping.

Comparing the magnitude of velocity and streamlines path in horizontal sections with occurrence of secondary currents in radial sections, it was revealed that the flow in the main spiral direction plays a higher role on removal efficiency.

Notation

B = Width of the inlet canal (m).
 d = Diameter of the basin (m).
 d_{50} = Median size of sediment particles (m).
 d_o = Diameter of central orifice (m).
 g = Acceleration due to the gravity (m/s^2).
 H = Height of circular basin (m).
 h = Vertical distance from the basin floor (m).
 h_1 = Distance between diaphragm and inlet canal bed (m).

h_2 = Chamber depth at its periphery from inlet canal bed (m).
 h_p = Depth of flow at the periphery of vortex basin (m).
 k_l = Mobility factor
 k_o = Coefficient related to the configuration of vortex settling basin
 L_l = Length of overflow weir (m).
 Q_i = Entrance flow discharge (m^3/s).
 Q_o = Flushing discharge (m^3/s).
 Q_r = Radial near bed discharge (m^3/s).
 Q_s = Overflow discharge (m^3/s).
 $Q_w = Q_o + K \cdot Q_s$ = weighted discharge (m^3/s).
 r = Radial distance from center of basin (m).
 R = Radius of basin (m).
 r_o = Radius of flushing orifice (m).
 S = Bed slope of conveyances canal (%).
 S_c = Radial slope of the basin floor (%).
 $V_{\theta o}$ = Tangential velocity at $r = r_o$ (m/s).
 $W = 4Q_s/\pi d^2$ = vertically upward velocity at center of basin (m/s).
 Z_h = Difference between bed levels of overflow weir and vortex basin (m).
 γ_f = Specific weight of fluid (N/m^3).
 γ_s = Specific weight of sediment particles (N/m^3).
 η_h = Hydraulic efficiency of vortex settling basin (%).
 η_o = Removal efficiency of vortex settling basin (%).
 θ = Angular distance (degree).
 ν = Kinematics viscosity of fluid (m^2/s).
 ω = Fall velocity of sediment particles in quiescent water (m/s).
 ω_i = Weight of sediment fed into the basin (kg).
 ω_o = Dry weight of the sediment, flushed out through the bottom orifice (kg).

REFERENCES

1. Gard, R.J. and K.G. Ranga Raju, 2000. Mechanics of sediment transportation and alluvial stream problems, 3rd Edn. New Age International, New Dehli, India.
2. Keshavarzi, A.R. and A.R. Gheisi, 2006. Trap efficiency of vortex settling basin for exclusion of fine suspended particles in irrigation canals. J. Irrigation. Drainage. Engng., 55(4): 419-434.
3. Ziaei, A.N., M. Javan and A.L. Keshavarzi, 2001, A new feature of vortex settling basin (VSB). In Proceedings of International Conference on Hydraulic Structures, Kerman, Iran, 3: 41-54.
4. Athar, M., U.C. Kothyari and R.J. Garde, 2002. Sediment removal efficiency of vortex chamber type sediment extractor. J. Hyd. Engng, ASCE, 128(2): 1051-1059.

5. Mashauri, D.A., 1986. Modeling of vortex settling chamber for primary clarification of water, Ph.D. thesis, Tampere University of Technology, Tampere, Finland, pp: 217.
6. Paul, T.C., S.K. Sayal, V.S. Sakhanja and G.S. Dhillon, 1991. Vortex settling chamber design considerations. *J. Hyd. Engng*, 117(2): 172-189.
7. Velioglu, S.G., 1972. Vortex type sedimentation tank. M.Sc Engng. Thesis, Bogasiqi University, Turkey.
8. Salakhov, F.S., 1975. Rotational design and methods of hydraulic calculation of load-controlling water intake structures for Mountain Rivers. *Proceedings of Ninth Congress of the ICID, Moscow, Soviet Union*, pp: 151-161.
9. Cecen, K. and M. Bayazit, 1975. Some laboratory studies of sediment controlling structures calculation of load-controlling water intake structures for Mountain Rivers. *Proceedings of the Ninth Congress of the ICID, Moscow, Soviet Union*, pp: 107-110.
10. Sullivan, R.H., M.M. Cohn, J.E. Ure, F. Parkinson, G. Galina, R.R. Boericke, C. Kock and P. Zielinki, 1978. The swirl primary separator; development and pilot demonstration. US Environmental Protection Agency, Cincinnati, Report No. EPA-600/2-78-122.
11. Curi, K.V., I.I. Esen and S.G. Velioglu, 1979. Vortex type solid liquid separator. *Progress in Water Technol.*, 7(2): 183-190.
12. Ogihara, K. and S. Sakaguchi, 1984. New system to separate the sediment from the water flow by using the rotating flow, In *Proceedings of Fourth Congress of the Asia and Pacific Division, International Association of Hydrological Research, Chiang Mai, Thailand*, pp: 753-766.
13. Sanmuganthan, K., 1985. A note on outlet pipe design for circulation chamber silt extractor. *Hydraulic Research Wallingford Limited, Wallingford, England, Report*, pp: 87.
14. Zhou, Z., C. Wang and J. Hou, 1989. Model study on flushing cone with strong spiral flow. In *Proceedings, 4th International Symposium on River Sedimentation, Beijing*, pp: 1213-1219.
15. Zhou, Z., J. Hou and Yi. Tang, 1997. Flow field measurement of sand funnel and its influence on sediment transport. In *Proceedings, 27th Congress, IAHR, San Francisco*.